



Kahramanmaraş Sütçü İmam University

Journal of Engineering Sciences



Geliş Tarihi : 20.12.2022
Kabul Tarihi : 26.02.2023

Received Date : 20.12.2022
Accepted Date : 26.02.2023

THE COMPARISON OF THE EFFECTS OF THRESHOLDING METHODS ON SEGMENTATION USING THE MOTH FLAME OPTIMIZATION ALGORITHM

EŞİKLEME METOTLARININ SEGMENTASYON ÜZERİNDEKİ ETKİLERİNİN GÜVE ALEV OPTİMİZASYONU ALGORİTMASI KULLANILARAK KARŞILAŞTIRILMASI

Murat KARAKOYUN (ORCID: 0000-0002-0677-9313)

Necmettin Erbakan University, Department of Computer Engineering, Konya, Turkey

*Corresponding Author: Murat KARAKOYUN, mkarakoyun@erbakan.edu.tr

ABSTRACT

Segmentation is an important preprocessing step that directly affects the success in image processing applications. There are many methods and approaches used for the segmentation process. Thresholding is a frequently used approach among these methods. There are several suggested approaches to thresholding. In this study, six different thresholding approaches were used as the fitness functions using the moth flame algorithm and the results obtained from these approaches were compared. In experimental studies, seven different threshold levels of 10 different images were studied. In comparisons made with three different metrics, it was seen that the Otsu method was generally more successful. It has also been observed that the minimum cross entropy and Renyi entropies can be used as alternatives.

Keywords: Kapur, moth flame optimization, Otsu, segmentation, thresholding

ÖZET

Segmentasyon görüntü işleme uygulamalarında başarıyı doğrudan etkileyen önemli bir ön işlem adıdır. Segmentasyon süreci için kullanılan birçok yöntem ve yaklaşım mevcuttur. Eşikleme bu yöntemler içerisinde sıklıkla kullanılan bir yaklaşımdır. Eşikleme için önerilen birçok yaklaşım bulunmaktadır. Bu çalışmada moth flame algoritması kullanılarak altı farklı eşikleme yaklaşımı uygunluk fonksiyonu olarak kullanılmış ve bu yaklaşımlardan elde edilen sonuçlar karşılaştırılmıştır. Deneysel çalışmalarda 10 farklı görüntünün yedi farklı eşik seviyesi üzerinde çalışılmıştır. Üç farklı metrik ile yapılan kıyaslamalarda Otsu metodunun genel olarak daha başarılı olduğu görülmüştür. Ayrıca minimum cross entropy ve Renyi entropilerinin de alternatif olarak kullanılabilceği gözlemlenmiştir.

Anahtar Kelimeler: Kapur, güve alev optimizasyonu, Otsu, segmentasyon, eşikleme

INTRODUCTION

Segmentation is a very important and difficult step for image processing applications. A successful segmentation or an unsuccessful segmentation result directly affects the success of the image processing application. Therefore, this step needs to be handled and performed carefully. The segmentation process is applied to make the image more understandable for the next stages and to prepare it for further processing. The main purpose at this stage is to group the pixels in the image according to their similarities and to ensure that the image is represented with fewer pixel groups. After this stage, it is easier to separate the objects in the image from the background. Because segmentation is such a difficult and important process, researchers have developed and proposed different approaches. Clustering-based (Karakoyun et al., 2017b), edge-based (Priyadharsini & Sharmila, 2019), region-based (Yupeng Li et al., 2020), thresholding-based (Selçuk et al., 2017) etc. are the most known approaches that used for image segmentation. When compared with the others, thresholding methods are widely used because of its simplify and practical applicability (Cai et al., 2022; Karakoyun et al., 2017a; Karakoyun et al., 2021).

The aim of the thresholding methods is to separate the images into similar pixel regions with the selected threshold values. The histogram of the image plays an important role when the threshold values are selected. The number of thresholds is a value used to categorize thresholding methods. According to the number of threshold values, these methods categorized as bi-level and multi-level thresholding. In bi-level thresholding, there is only one threshold value that separate the image into two classes. The pixels under the threshold value are assigned as 0 (black) and the pixels greater than threshold value are assigned as 1 (white). So that a binary image is generated when bi-level thresholding is applied to the image. On the other hand, more than one threshold value is needed when multi-level thresholding is used. Although thresholding approach is effective and simple, there is a complex problem with the selection of the threshold value(s). Especially when the number of thresholds is high, this complexity raises more (Abdel-Basset et al., 2022; Chen et al., 2022; Houssein et al., 2022; Karakoyun et al., 2021). To handle and solve this problem, many methods like Otsu (Otsu, 1979), Kapur (Kapur et al., 1985), Tsallis (De Albuquerque et al., 2004), Renyi (Sahoo et al., 1997) etc. have been proposed for the image thresholding. These approaches generally work based on variance or entropy and measure the quality of selected threshold values. Since the thresholding problem is a combinatorial problem, its complexity is quite high. It is therefore very difficult to consider all combinations individually for threshold values within an acceptable time limit. It is almost impossible, especially in cases where the number of thresholds is high. In the course of time, metaheuristic algorithms have started to be used in order to get rid of this time complexity and to obtain sensible solutions within an acceptable time. Metaheuristic algorithms use thresholding methods as fitness functions and try to optimize these functions to determine the best threshold values. When we look at the literature, it is seen that there are many studies that have been put forward with this approach. It is almost impossible in terms of time and effort to consider and examine all of these studies. For this reason, some of these studies were analyzed within the scope of related works.

Ryalat et al. (Ryalat et al., 2022) used Harris hawks optimization (HHO) algorithm to segment chest images of covid-19 patients. They used the Otsu thresholding method as a fitness function. The performance of the HHO algorithm was compared with the Otsu method with three metrics to calculate the quality of the segmented images. On the other hand, comparison was made in terms of time and it was stated that the HHO algorithm was in advance in terms of speed. Günay and Taze (Günay & Taze, 2022) performed segmentation for the detection of cytoplasm in multiple myeloma plasma cells. They used the Otsu method as the thresholding method. They stated that the deep learning supported U-net network approach they used generally achieved satisfactory results. Zhao et al. (Zhao et al., 2021) proposed a diffusion association slime mould algorithm (DASMA) for multi-level image thresholding. The suggested algorithm was applied on the images taken from Berkeley dataset and CT images by using Renyi's entropy as a fitness function. They compared the performance of the DASMA with the performance of the several algorithms. They declared that the proposed algorithm has successful results on image segmentation process. Xing and He (Xing & He, 2021) used marine predators algorithm (MPA) on segmentation of the infrared images. The authors handled the segmentation as a multi-objective problem by using 9D Kapur as a fitness function. The aim of the work is to detect the fault regions in the infrared images of the power systems by using a boost MPA (BMPA). The performance of the proposed BMPA was compared with the performances of the other multi-objective algorithms. It has been stated that the BMPA is successful to diagnosis the faults in images and has better performance than the compared algorithms. Ma and Yue (Ma & Yue, 2022) improved a method based on the whale optimization algorithm (WOA) to solve the multi-level thresholding problem. They applied their method which is named as RAV-WOA on a set of benchmark images (include gray and color samples) by using Otsu's between class variance as an objective function. The performance comparison was made between the proposed method and several metaheuristic algorithms with the

PSNR and MSSIM metrics. They stated that the RAV-WOA method has better results than the other algorithms. Huang et al. (Huang et al., 2021) applied fruitfly optimization algorithm (FOA) for a thresholding segmentation problem. They used three benchmark images as dataset and Otsu's method as an objective function. They compared the performance of their algorithm with the classical Otsu's method. Fitness value and speed of the algorithms' used as comparison metrics. They stated that their algorithm has equal fitness values but is faster than classical Otsu's method. Kalyani et al. (Kalyani et al., 2020) used exchange market algorithm (EMA) with minimum cross entropy (MCE) for image segmentation. They applied EMA on optimization of benchmark functions and segmentation of brain images with different threshold levels. They specified that the EMA has better performance than compared algorithms on different metrics. Raj et al. (Raj et al., 2019) employed differential evolution (DE) algorithm with Tsallis-Fuzzy entropy method for an image segmentation problem. The performance of the Tsallis-Fuzzy approach was compared with the Shannon and Tsallis methods. Besides, a performance comparison of the DE with Tsallis-Fuzzy was done with the performance of the different state-of-the-art algorithms. SSIM, PSNR, SNR and statistical tests were used as performance comparison metrics. They marked that the proposed algorithm has better results than the other algorithms. Koc et al. (Koc et al., 2018) applied GWO algorithm with the Otsu thresholding approach on six benchmark images for multilevel image thresholding problem. They applied the GWO algorithm with four (2, 3, 4, 5) different threshold levels and compared the performance of the algorithm with five metaheuristic algorithms. According to the experimental results they stated that the GWO algorithm was generally more successful than the other algorithms. Naidu et al. (Naidu et al., 2018) selected Shannon entropy and firefly algorithm (FA) for a thresholding image segmentation problem. The FA applied on benchmark images and a performance comparison was done with three metaheuristic algorithms by using SSIM, PSNR, error rate and CPU time metrics. The experimental results of the study show that the performance of the FA is better than the performance of the other algorithms. Bhandari et al. (Bhandari et al., 2015b) proposed a variant of the cuckoo search (CS) algorithm for thresholding segmentation problem. In the study, Tsallis entropy was used as a fitness function and the proposed algorithm was applied on satellite and benchmark images. The performance of the proposed algorithm was compared with the performance of the several metaheuristic algorithms on different metrics. The authors stated that the proposed algorithm has better results than the other algorithms.

In this study, it is aimed to measure the success of thresholding methods by using the recently proposed MFO algorithm. For this purpose, six thresholding approaches (Otsu, Kapur, Renyi, Tsallis, MCE, Shannon) were used on 10 images with different features. The MFO algorithm was applied separately using each of these approaches as a fitness function. Seven different threshold levels were used for comprehensive analysis. In addition, three different comparison metrics (PSNR, SSIM, FSIM) were used to evaluate the results from different perspectives. The successful thresholding approach was determined by making a detailed analysis on the basis of threshold level and comparison metric.

THRESHOLDING PROBLEM

Thresholding is a very popular and simple method for an image segmentation problem. The thresholding method is generally applied on the grayscale images by using their histogram. If the threshold number is used as categorization criteria, thresholding transaction can be classified into two sections: bi-level and multi-level thresholding. In bi-level thresholding, only one threshold value divides the image into two classes. As a result of the bi-level image thresholding, the gray scale image is converted to a binary image that includes only 0 and 1 pixels. In gray scale image, the pixel values under threshold are marked as zero and others are assigned as one. On the other hand, in multi-level thresholding, the threshold number is greater than one. In this type of thresholding, an image that has multi classes is achieved as output image. Let's think that I is the image that will divided into m ($C_1, C_2 \dots C_m$) classes by using T ($T_1, T_2 \dots T_{m-1}$) threshold values. Equation (1) shows the separation of the image into m classes by using $m-1$ threshold values (Bhandari et al., 2015a, 2015b; Ishak, 2017; Karakoyun et al., 2017a; Karakoyun et al., 2021).

$$\begin{aligned}
 C_1 &= \{g(x, y) \in I | 0 \leq g(x, y) \leq T_1 - 1\} \\
 C_2 &= \{g(x, y) \in I | t_1 \leq g(x, y) \leq T_2 - 1\} \\
 &\vdots \\
 C_i &= \{g(x, y) \in I | t_i \leq g(x, y) \leq T_{i+1} - 1\} \\
 &\vdots \\
 C_m &= \{g(x, y) \in I | T_{m-1} \leq g(x, y) \leq L\}
 \end{aligned} \tag{1}$$

where L is the maximum pixel value of the gray scale image and generally is 256.

MOTH FLAME OPTIMIZATION

The MFO (Mirjalili, 2015) algorithm that is inspired by the nocturnal flight strategy of moths and proposed by Mirjalili. In the algorithm, moths have a specific flying mechanism which uses the moon light with a stable angle. The mechanism that they use for navigation is called as transverse orientation. This strategy provides an effective and comfort travelling in a long straight distance. But, the moths are affected from artificial lights and try to act similar with having an angle with this artificial light. The flying of the moths by keeping a constant angle between them and the light causes a spiral movement. In this case, it can be observed that the cross-direction strategy is only effective for distant lights such as moonlight. Figure 1 presents the spiral flying of the moths around the light (Karakoyun & Özkış, 2021; Yu Li et al., 2020; Mirjalili, 2015).

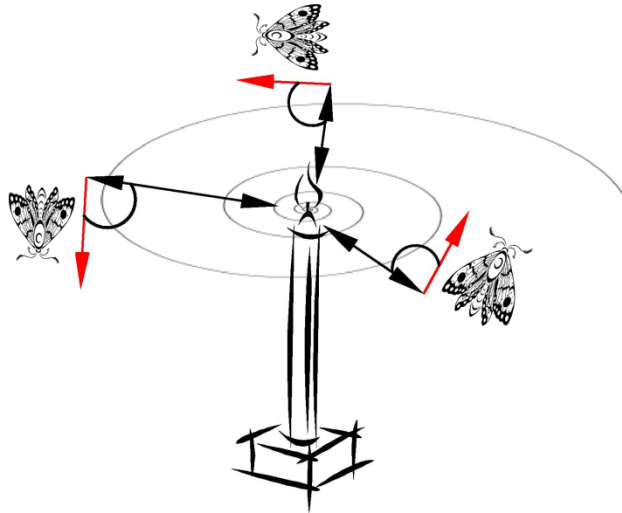


Figure 1. Spiral Flying of Moths Around the Light

Figure 1 clearly shows that the moths eventually close towards the light source. The MFO algorithm was mathematically modelled and developed by inspired the behavior of moths with the light source. Like other metaheuristic algorithms, the MFO is also a population based and iterative algorithm. The algorithm basically consists of moths and flames. While each moth in the population represents a possible solution, each variable that constitutes the position of the moth represents one dimension of the problem. Let's think that N is the population size and D is the dimension of the problem then the population of the moths can be represented with a matrix as follow:

$$M = \begin{bmatrix} m_{11} & \cdots & m_{1D} \\ \vdots & \ddots & \vdots \\ m_{N1} & \cdots & m_{ND} \end{bmatrix} \quad (2)$$

here M represents the population of the moths. There is an array of the fitness values related with the positions. The array of the fitness values (OM) can be represented as follow:

$$OM = \begin{bmatrix} OM_1 \\ OM_2 \\ \vdots \\ OM_N \end{bmatrix} \quad (3)$$

The moths in population use an updating process to improve their position. In updating process each moth uses a reference flame. It is expected to avoid the local optima and to make an effective search by feeding from different flames in position update phase. The position of the flames has the same size as the moths and the flames have an

array of fitness values. The position and fitness values of the flames are represented in Eq. (4) and Eq. (5), respectively.

$$F = \begin{bmatrix} f_{11} & \cdots & f_{1D} \\ \vdots & \ddots & \vdots \\ f_{N1} & \cdots & f_{ND} \end{bmatrix} \quad (4)$$

$$OF = \begin{bmatrix} OF_1 \\ OF_2 \\ \vdots \\ OF_N \end{bmatrix} \quad (5)$$

As mentioned above, the moths and flames are the same in terms of presentation and structure. The difference between them is the way they are treated within the population. The position of the moths is updated at each iteration, while the best positions ever found are selected as flames. The flames are selected at each iteration step from the best positions obtained in the previous iteration step. On the other hand, moths are assisted by a flame as a reference point during the position update process. Figure 2 shows the flame selection strategy of the MFO algorithm.

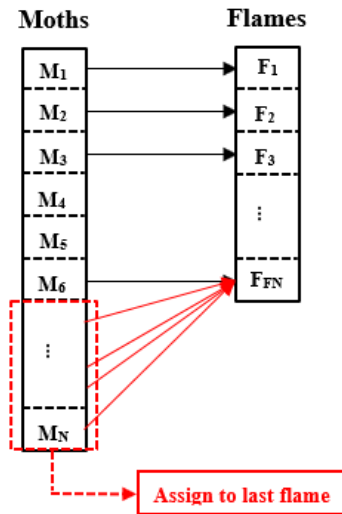


Figure 2. Reference Flame Selection for Moths

The mathematical model of the position update that inspired by Fig. 1 is given in Eq. (6).

$$M_i = D_i * e^{bt} * \cos(2\pi t) + F_j \quad (6)$$

$$D_i = |F_j - M_i| \quad (7)$$

Here $M_i = (m_{i1}, m_{i2}, \dots, m_{iD})$ and $F_j = (f_{j1}, f_{j2}, \dots, f_{jD})$ are the positions of the i th moth and j th flame respectively, D_i is the distance between i th moth and related j th flame and calculated by Eq. (7), t is a number generated randomly in $[-1, 1]$ and generated by using Eq. (8) and b is a constant value to determine the form of the logarithmic spiral.

$$t = (a - 1) * rand + 1 \quad (8)$$

$$a = -1 + k * \left(-\frac{1}{K}\right)$$

The current iteration number is k , and K is the maximum iteration number.

In the mechanism of the algorithm, the number of the flames is decreased for each iteration by using Eq. (9) as follow:

$$flame_number = round\left(N - k * \frac{N-k}{K}\right) \quad (9)$$

where N is the maximum flame number that is equal to population size at the beginning of the algorithm.

The MFO algorithm has a similar processing mechanism as other metaheuristic algorithms. The parameters of the algorithm must be set in first step. Then a random population is generated within the boundary of the solution space. For each moth (position) in population, fitness values are calculated and the flames are assigned. The main loop of algorithm is started. In this loop, for each moth the position update procedure works, the number of the flames is updated and best position is saved for each iteration step. The loop continues until the termination criterion is met (Karakoyun & Özkış, 2021; Mirjalili, 2015; Shehab et al., 2020). Figure 3 shows the main steps of the MFO algorithm.

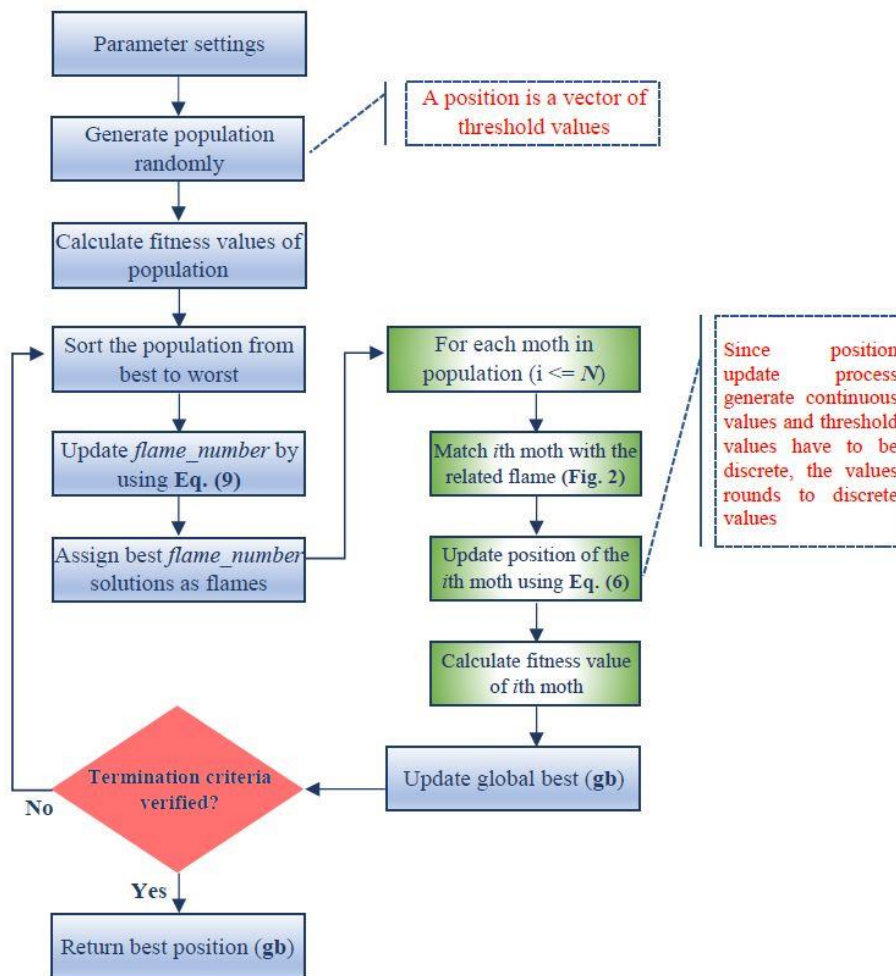


Figure 3. The Main Steps of the MFO Algorithm

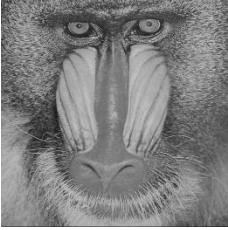







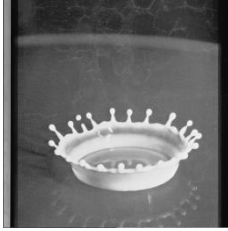

EXPERIMENTAL STUDY

In this section, firstly, the images handled for thresholding were presented. Then the thresholding methods were explained in a short view. Finally, experimental results were presented comparatively.

Dataset Images

In this paper, 10 well-known benchmark images which are mostly used for image segmentation in the literature were handled. The sizes of the images that are gray scale are different from each other; however, bit depth of all images is 8. For this reason, the value that each pixel in the images can take is between 0-255. The benchmark images are presented in Table 1.

Table 1. The Images Used for Thresholding Segmentation

Baboon (I ₁)	Barbara (I ₂)	Boats (I ₃)	Bridge (I ₄)	Camera (I ₅)
				
Columbia (I ₆)	Couple (I ₇)	Lena (I ₈)	Milkdrop (I ₉)	Peppers (I ₁₀)
				

Thresholding Methods

The thresholding is a simple and successful approach for image segmentation. There are many methods used in thresholding segmentation. These methods are used to measure how appropriate the chosen threshold value (or values) is. In this study, the selected algorithm was tested using the thresholding methods given below.

Otsu's Method

Otsu's (Otsu, 1979) method is a popular and useful approach for thresholding. This approach is used to calculate the variance within the pixel classes separated by the threshold values (Karakoyun et al., 2017a; Satapathy et al., 2018). The main purpose of the algorithms is to determine the threshold values that minimize the total variance within the class by using Otsu's within class variance which is presented in Eq. (10).

$$\sigma_w^2 = \sum_{j=1}^m w_j \sigma_j^2 \quad (10)$$

Here w_j and σ_j^2 are the gray level distribution and the variance of the j th class, respectively.

$$w_j = \sum_{i=T_{j-1}+1}^{T_j} P_i \quad (11)$$

$$\sigma_j^2 = \sum_{i=T_{j-1}+1}^{T_j} (i - u_j)^2 P_i / w_j \quad (12)$$

$$P_i = \frac{n_i}{N} \quad (13)$$

$$u_j = \sum_{i=T_{j-1}+1}^{T_j} i * P_i / w_j \quad (14)$$

P_i is the probability of the i th gray level and u_j is the mean value of the j th class. n_i is the number of pixels at i th gray level and N is number of the all pixels in image.

Kapur Entropy

Kapur entropy is another famous and simple method for thresholding. This approach works based on the entropy. The main purpose is to maximize the entropy of the separated regions by the threshold values. Assume that I is a grayscale image with N number of pixels and L ($0 < L < 255$) gray level. The number of the pixels at i th gray level is n_i and the probability of i th pixels in the image is $p_i = n_i / N$. Kapur method purposes to maximize total entropy given in Eq. (15) (Kapur et al., 1985; Karakoyun et al., 2021; Tuba et al., 2017).

$$f(T) = \sum_{i=0}^n H_i \quad (15)$$

The H_i entropies are calculated by the following equation:

$$\begin{aligned} H_0 &= - \sum_{i=0}^{T_0-1} \frac{p_i}{\omega_0} \ln \frac{p_i}{\omega_0}, \quad \omega_0 = \sum_{i=0}^{T_0-1} p_i \\ H_1 &= - \sum_{i=T_0}^{T_1-1} \frac{p_i}{\omega_1} \ln \frac{p_i}{\omega_1}, \quad \omega_1 = \sum_{i=T_0}^{T_1-1} p_i \\ &\vdots \\ H_n &= - \sum_{i=T_{n-1}}^{L-1} \frac{p_i}{\omega_n} \ln \frac{p_i}{\omega_n}, \quad \omega_n = \sum_{i=T_{n-1}}^{L-1} p_i \end{aligned} \quad (16)$$

Except the most commonly used Otsu and Kapur methods, other approaches used are Renyi (Sahoo et al., 1997), Tsallis (De Albuquerque et al., 2004), Minimum Cross Entropy (MCE) (Pal, 1996) and Shannon (Naidu et al., 2018; Shannon, 1948) approaches. Among these approaches, only the Otsu method is variance-based, while the rest are entropy-based. More details of other approaches can be found in reference studies.

Experimental Results

In the experiments, 10 benchmark images presented in Table 1 were used for the segmentation. MFO algorithm was applied on images by using six different thresholding methods as the objective function. For each method, algorithm was applied 20 times and average results of 20 runs were presented in result tables with three metrics. In this section, first, comparison metrics were introduced and then the experimental results were presented.

Comparison Metrics

In this study, to measure the quality of the segmented images three comparison metrics were used: Peak signal-to-noise ratio (PSNR), structural similarity index measure (SSIM) and featured similarity index measure (FSIM).

PSNR is the most famous metric to measure the quality of the segmentation process. It is used to calculate the rate between the maximum possible signal power and the power of the deflecting noise that affects the quality of its representation. Because of the signals having a very wide dynamic range the PSNR is usually calculated as the logarithm term of decibel scale. PSNR value depends on the mean squared error (MSE) between the original (or if there is ground truth image) and segmented image. So, a higher PSNR value is wanted and a smaller value means a bad segmentation result (Hore & Ziou, 2010; Sara et al., 2019). Equation (17) shows the PSNR value between f -grey scale image and g -segmented image.

$$PSNR = 10 \log_{10}(K^2 / MSE(f, g)) \quad (17)$$

$$MSE(f, g) = \frac{1}{mn} \sum_{i=1}^m \sum_{j=1}^n (f_{ij} - g_{ij})^2 \quad (18)$$

Here $m \times n$ is the size of the both f and g images, K is the maximum pixel value of the images and is 255 (since bit depth of image is 8).

SSIM is another popular metric to calculate the similarity between the source and destination image. The SSIM is evaluated by using three main elements named luminance, contrast and structure. The SSIM takes a value between 0 and 1 according to the similarity between images. A higher value for the metric is wanted that means a better quality of segmentation. The mathematical model of the SSIM can be expressed as follow (Brooks et al., 2008; Hore & Ziou, 2010; Sara et al., 2019; Wang et al., 2004):

$$SSIM(f, g) = [l(f, g)]^\alpha * [c(f, g)]^\beta * [s(f, g)]^\gamma \quad (19)$$

where l is the luminance that compares brightness between f and g images, c is the contrast that compares the difference between the brightest and darkest areas of the f and g images, s is the structure compares the luminance pattern of the f and g images, and α , β and γ are the constants numbers that have positive values. The luminance, contrast and structure between f and g images can be calculated by using Eq. (20).

$$l(f, g) = \frac{2 \mu_f \mu_g + C_1}{\mu_f^2 + \mu_g^2 + C_1}$$

$$c(f, g) = \frac{2 \sigma_f \sigma_g + C_2}{\sigma_f^2 + \sigma_g^2 + C_2} \quad (20)$$

$$s(f, g) = \frac{\sigma_{fg} + C_3}{\sigma_f \sigma_g + C_3}$$

Here μ_f and μ_g are the mean of images, σ_f and σ_g are standard deviation of the images, and σ_{fg} is the cross covariance of the f and g images.

FSIM is a popular metric that calculate the similarity between two images by mapping the features. The metric needs phase congruency (PC) and gradient magnitude (GM) of the images. PC points on the features of the image in the domain frequency and it is invariant to contrast. On the other hand, convolution masks are used to calculate the GM value of an image. For f and g images, PC_f and PC_g are the phase congruency maps, respectively and G_f and G_g are the magnitude gradient maps, respectively (Sara et al., 2019; Zhang et al., 2011). Then FSIM value between two images can be calculated by using Eq. (21).

$$FSIM(f, g) = [S_{PC}(f, g)]^\alpha * [S_G(f, g)]^\beta \quad (21)$$

$$S_{PC}(f, g) = \frac{2 PC_f PC_g + T_1}{PC_f^2 + PC_g^2 + T_1} \quad (22)$$

$$S_G(f, g) = \frac{2 G_f G_g + T_2}{G_f^2 + G_g^2 + T_2} \quad (23)$$

α and β are used to set the correlative importance of GM and PC features and used as $\alpha = \beta = 1$ based on the referenced work. T_1 and T_2 are positive constant values and used as 0.85 and 160 based on the referenced work. As a result, FSIM takes a value between 0 and 1. A higher value is wanted for a better segmentation result.

PSNR Results

PSNR is a metric that calculates the quality of the segmented image and a higher value is wanted for this metric. Table 2 shows the PSNR metric-based results of six thresholding methods. The MFO algorithm was applied on 10 images with seven threshold levels (2, 4, 6, 8, 10, 12, 15). In this case, a total of 70 cases emerged in the experimental studies. In these 70 cases, Otsu method had 68 best average results and MCE had 2 best average results. In addition to the numerical best cases, when the results are examined in detail, it can be said that the MCE and Renyi methods

are the most successful approaches after the Otsu method. However, Shannon entropy can be considered as the most unsuccessful approach according to PSNR metric-based results. On the other hand, Tsallis and Kapur took their place in the results of this metric with an average success.

Table 2. PSNR Metric-based Results of the Methods

Method	#TH	I ₁	I ₂	I ₃	I ₄	I ₅	I ₆	I ₇	I ₈	I ₉	I ₁₀
Otsu	2	25.62	22.33	24.67	21.47	24.40	23.51	22.80	24.27	22.27	22.45
	4	29.57	26.61	28.45	25.74	27.88	27.84	26.66	29.38	26.83	26.79
	6	32.13	29.16	31.13	28.59	30.73	30.71	29.61	32.28	30.15	29.73
	8	34.02	31.29	33.32	30.69	33.08	32.86	31.74	33.98	32.05	31.89
	10	35.59	32.83	35.11	32.16	34.69	34.62	33.38	35.50	33.81	33.40
	12	36.72	34.19	36.37	33.69	35.89	35.69	34.71	36.64	35.04	34.79
	15	38.38	35.93	37.79	35.41	37.37	37.43	36.26	38.13	36.57	36.45
Kapur	2	21.34	21.37	20.80	21.28	18.18	22.74	21.61	21.06	21.59	22.18
	4	26.38	26.35	24.71	25.38	26.93	24.85	25.41	24.59	24.98	25.06
	6	28.11	28.56	28.87	27.67	28.22	28.44	27.33	28.66	28.04	27.70
	8	30.14	30.12	30.83	29.34	30.78	30.22	29.79	30.61	30.25	30.32
	10	31.49	31.54	32.13	29.94	32.41	31.52	31.55	31.97	31.56	32.17
	12	32.93	32.99	33.41	30.69	33.74	33.00	32.86	33.08	32.91	33.36
	15	34.69	34.61	34.87	30.85	35.49	34.89	34.20	34.85	34.48	34.89
Renyi	2	25.50	22.06	24.48	21.42	23.18	23.39	22.69	24.24	22.07	21.83
	4	29.21	26.40	28.18	25.72	27.38	27.68	26.46	29.05	26.72	26.51
	6	31.85	28.98	31.04	28.44	30.60	30.58	29.35	31.77	29.79	29.57
	8	33.80	31.05	33.23	30.43	32.85	32.75	31.53	33.58	31.81	31.69
	10	35.43	32.73	34.93	32.15	34.35	34.20	33.09	35.15	33.58	33.29
	12	36.58	34.11	36.14	33.59	35.56	35.59	34.39	36.54	34.90	34.62
	15	37.96	35.78	37.69	35.27	37.04	36.60	35.79	37.86	36.44	36.31
Tsallis	2	22.16	20.39	21.03	19.50	16.78	20.80	19.92	21.90	18.71	19.62
	4	26.17	23.42	24.75	21.49	22.36	24.26	23.07	25.59	23.32	23.96
	6	27.08	25.60	21.17	15.68	25.55	26.23	22.06	27.81	24.76	22.12
	8	28.07	24.86	19.63	13.94	26.84	27.67	18.42	27.72	26.41	16.78
	10	29.00	23.32	18.38	13.71	27.82	28.68	16.48	29.49	27.79	16.07
	12	29.89	24.13	17.21	13.47	27.82	29.36	16.47	28.78	28.10	17.07
	15	30.22	20.35	18.89	13.51	30.35	29.80	15.86	30.15	29.76	19.27
MCE	2	25.49	22.08	24.01	21.07	23.79	23.04	22.46	24.13	21.98	22.08
	4	29.42	25.89	27.67	24.89	27.41	27.49	26.20	29.28	26.32	26.51
	6	31.94	28.68	30.26	27.91	29.95	30.44	29.23	32.00	29.51	28.98
	8	33.81	30.78	32.79	29.53	32.24	32.58	31.06	33.81	31.88	31.10
	10	35.32	32.43	34.50	31.47	34.09	34.26	32.96	35.45	33.51	32.99
	12	36.78	33.86	35.83	32.94	35.33	35.63	34.25	36.67	34.84	34.20
	15	38.15	35.44	37.51	34.90	36.95	37.30	35.94	38.05	36.45	35.97
Shannon	2	23.97	18.72	21.18	13.41	14.09	20.01	18.92	16.70	16.57	16.43
	4	24.38	18.77	22.78	13.46	20.74	19.60	18.92	16.66	16.50	17.92
	6	24.06	18.99	23.38	13.52	23.76	19.21	18.98	16.77	16.54	17.97
	8	24.22	19.18	23.20	13.53	25.03	19.13	19.03	17.46	16.56	19.69
	10	24.38	19.28	23.79	13.54	26.59	18.93	19.07	17.42	16.56	19.95
	12	24.73	19.11	24.00	13.54	26.34	18.88	19.08	18.69	16.63	20.35
	15	24.74	19.81	24.34	13.58	27.37	18.78	19.06	18.35	19.36	20.61

SSIM Results

This metric measures the quality of the segmented images based-on structural properties. A value between 0 and 1 is generated as a result of this metric and a higher value is wanted for a better segmentation result. As mentioned above, there are 70 cases of experiments that needed to be handled. Table 3 shows the average results of the methods based-on SSIM metric. According to these results, The Otsu method showed the best average results in 61 of the 70 cases, showing that it was the most successful approach in this metric as well. The success of the Otsu method was followed by MCE, which was successful in 44 of the 70 cases. The Renyi method, which achieved the best success average of

19, came in third place. When the results in Table 3 is examined in general, it is seen that Kapur and Tsallis approaches have achieved an average success, as in the PSNR metric. Shannon's entropy is also behind in this metric in terms of average success.

Table 3. SSIM Metric-based Results of the Methods

Method	#TH	I ₁	I ₂	I ₃	I ₄	I ₅	I ₆	I ₇	I ₈	I ₉	I ₁₀
Otsu	2	0.77	0.71	0.77	0.64	0.80	0.77	0.66	0.73	0.72	0.67
	4	0.87	0.80	0.84	0.79	0.85	0.83	0.76	0.81	0.76	0.73
	6	0.92	0.84	0.88	0.86	0.89	0.87	0.84	0.86	0.81	0.79
	8	0.94	0.87	0.90	0.90	0.91	0.90	0.87	0.88	0.84	0.83
	10	0.96	0.90	0.92	0.92	0.93	0.92	0.90	0.90	0.87	0.86
	12	0.97	0.91	0.94	0.94	0.94	0.93	0.92	0.92	0.89	0.89
	15	0.98	0.94	0.95	0.96	0.95	0.95	0.94	0.94	0.91	0.92
Kapur	2	0.62	0.68	0.68	0.62	0.68	0.75	0.62	0.70	0.72	0.65
	4	0.79	0.79	0.78	0.77	0.85	0.79	0.73	0.74	0.75	0.70
	6	0.83	0.83	0.85	0.83	0.87	0.84	0.77	0.80	0.77	0.75
	8	0.88	0.86	0.87	0.87	0.89	0.87	0.83	0.83	0.80	0.80
	10	0.90	0.88	0.89	0.88	0.90	0.88	0.86	0.85	0.82	0.83
	12	0.92	0.90	0.90	0.90	0.91	0.90	0.89	0.86	0.85	0.86
	15	0.94	0.92	0.92	0.90	0.93	0.92	0.91	0.89	0.87	0.89
Renyi	2	0.77	0.69	0.76	0.63	0.73	0.77	0.65	0.73	0.70	0.63
	4	0.86	0.79	0.82	0.79	0.84	0.83	0.75	0.80	0.76	0.71
	6	0.91	0.83	0.87	0.86	0.89	0.87	0.82	0.85	0.79	0.78
	8	0.94	0.87	0.90	0.89	0.91	0.90	0.86	0.87	0.83	0.82
	10	0.95	0.89	0.92	0.92	0.92	0.91	0.89	0.89	0.86	0.86
	12	0.96	0.91	0.93	0.94	0.93	0.93	0.91	0.91	0.88	0.88
	15	0.97	0.93	0.95	0.96	0.94	0.94	0.93	0.93	0.90	0.91
Tsallis	2	0.64	0.65	0.69	0.53	0.63	0.70	0.56	0.71	0.68	0.62
	4	0.78	0.73	0.78	0.62	0.77	0.77	0.67	0.76	0.73	0.69
	6	0.81	0.77	0.68	0.33	0.82	0.80	0.62	0.79	0.74	0.66
	8	0.83	0.74	0.63	0.24	0.85	0.83	0.50	0.80	0.76	0.57
	10	0.85	0.68	0.60	0.23	0.85	0.85	0.43	0.82	0.78	0.55
	12	0.87	0.71	0.58	0.22	0.86	0.86	0.43	0.81	0.78	0.57
	15	0.88	0.60	0.62	0.22	0.89	0.86	0.41	0.83	0.81	0.61
MCE	2	0.77	0.71	0.77	0.64	0.82	0.76	0.65	0.76	0.73	0.68
	4	0.87	0.78	0.83	0.78	0.86	0.83	0.75	0.81	0.77	0.74
	6	0.91	0.83	0.87	0.85	0.89	0.88	0.83	0.86	0.82	0.78
	8	0.93	0.87	0.90	0.89	0.91	0.90	0.86	0.88	0.84	0.82
	10	0.95	0.89	0.92	0.92	0.92	0.92	0.90	0.90	0.87	0.85
	12	0.96	0.91	0.93	0.94	0.94	0.93	0.92	0.92	0.89	0.88
	15	0.97	0.93	0.95	0.96	0.95	0.95	0.94	0.94	0.91	0.91
Shannon	2	0.71	0.59	0.69	0.22	0.50	0.70	0.54	0.62	0.66	0.57
	4	0.73	0.60	0.73	0.22	0.69	0.68	0.54	0.62	0.66	0.60
	6	0.72	0.60	0.76	0.22	0.76	0.66	0.55	0.62	0.66	0.60
	8	0.73	0.62	0.75	0.23	0.79	0.65	0.55	0.64	0.67	0.63
	10	0.73	0.62	0.77	0.23	0.82	0.64	0.56	0.63	0.66	0.64
	12	0.75	0.62	0.77	0.23	0.82	0.63	0.56	0.66	0.68	0.65
	15	0.75	0.64	0.78	0.23	0.84	0.63	0.56	0.65	0.72	0.66

FSIM Results

FSIM is last metric used in this work and calculates the similarity between source and destination images. For 70 cases, Otsu had 60 average best states, Renyi had 59 average best states and MCE had 42 average best states. On the other hand, Kapur entropy had 7 average best cases, where Tsallis and Shannon had no average best case in the experiments.

Table 4. FSIM Metric-based Results of the Methods

Method	#TH	I ₁	I ₂	I ₃	I ₄	I ₅	I ₆	I ₇	I ₈	I ₉	I ₁₀
Otsu	2	0.89	0.80	0.83	0.78	0.79	0.81	0.77	0.80	0.76	0.75
	4	0.95	0.89	0.91	0.89	0.86	0.89	0.89	0.89	0.84	0.85
	6	0.97	0.93	0.95	0.94	0.90	0.93	0.94	0.94	0.89	0.91
	8	0.98	0.95	0.97	0.96	0.93	0.96	0.96	0.96	0.92	0.95
	10	0.99	0.96	0.98	0.97	0.95	0.97	0.97	0.97	0.94	0.96
	12	0.99	0.98	0.98	0.98	0.96	0.98	0.98	0.98	0.96	0.98
	15	1.00	0.98	0.99	0.99	0.97	0.99	0.99	0.99	0.97	0.98
Kapur	2	0.76	0.78	0.71	0.77	0.70	0.78	0.73	0.72	0.76	0.74
	4	0.91	0.89	0.85	0.90	0.85	0.85	0.86	0.79	0.82	0.81
	6	0.94	0.92	0.92	0.94	0.88	0.91	0.91	0.88	0.87	0.88
	8	0.97	0.94	0.94	0.96	0.92	0.93	0.95	0.92	0.90	0.93
	10	0.98	0.95	0.96	0.96	0.93	0.95	0.97	0.94	0.92	0.95
	12	0.98	0.97	0.97	0.97	0.95	0.96	0.98	0.95	0.94	0.97
	15	0.99	0.98	0.98	0.97	0.96	0.98	0.98	0.97	0.96	0.98
Renyi	2	0.89	0.79	0.82	0.78	0.74	0.81	0.77	0.79	0.75	0.73
	4	0.96	0.89	0.91	0.90	0.85	0.89	0.88	0.89	0.84	0.85
	6	0.98	0.93	0.95	0.94	0.90	0.93	0.94	0.94	0.89	0.91
	8	0.99	0.95	0.97	0.96	0.93	0.96	0.96	0.96	0.92	0.95
	10	0.99	0.96	0.98	0.97	0.95	0.97	0.98	0.97	0.94	0.97
	12	0.99	0.98	0.98	0.98	0.96	0.98	0.98	0.98	0.96	0.98
	15	1.00	0.98	0.99	0.99	0.97	0.98	0.99	0.99	0.97	0.99
Tsallis	2	0.78	0.75	0.72	0.69	0.67	0.71	0.66	0.73	0.70	0.69
	4	0.90	0.82	0.84	0.76	0.77	0.82	0.80	0.81	0.79	0.79
	6	0.92	0.87	0.73	0.43	0.82	0.87	0.73	0.87	0.82	0.76
	8	0.94	0.84	0.68	0.33	0.86	0.90	0.57	0.86	0.85	0.63
	10	0.95	0.77	0.65	0.32	0.86	0.91	0.48	0.90	0.87	0.62
	12	0.96	0.80	0.61	0.30	0.87	0.92	0.49	0.89	0.87	0.64
	15	0.97	0.68	0.66	0.32	0.91	0.93	0.46	0.91	0.90	0.69
MCE	2	0.89	0.80	0.82	0.78	0.79	0.78	0.77	0.81	0.76	0.75
	4	0.95	0.88	0.90	0.88	0.87	0.88	0.88	0.88	0.84	0.85
	6	0.97	0.92	0.94	0.93	0.91	0.93	0.93	0.94	0.89	0.90
	8	0.98	0.95	0.96	0.95	0.93	0.95	0.96	0.96	0.92	0.93
	10	0.99	0.96	0.97	0.97	0.95	0.97	0.97	0.97	0.94	0.96
	12	0.99	0.97	0.98	0.98	0.96	0.98	0.98	0.98	0.96	0.97
	15	1.00	0.98	0.99	0.98	0.97	0.99	0.99	0.98	0.97	0.98
Shannon	2	0.84	0.69	0.73	0.28	0.58	0.69	0.62	0.61	0.70	0.62
	4	0.86	0.70	0.78	0.30	0.73	0.67	0.63	0.61	0.70	0.66
	6	0.85	0.71	0.80	0.32	0.78	0.65	0.63	0.61	0.70	0.65
	8	0.85	0.72	0.80	0.32	0.81	0.65	0.63	0.63	0.71	0.70
	10	0.86	0.73	0.81	0.33	0.84	0.65	0.64	0.63	0.70	0.71
	12	0.86	0.72	0.82	0.33	0.84	0.64	0.64	0.66	0.71	0.71
	15	0.86	0.74	0.83	0.34	0.86	0.64	0.64	0.65	0.75	0.72

Looking at the results in general, the Otsu method seems to be clearly successful in the PSNR metric. In addition, the MCE approach with Otsu in the SSIM metric draws attention in terms of success. The FSIM metric-based results show that the Otsu and Renyi methods achieve almost the same success. It is seen that another approach that draws attention in terms of success in this metric is MCE. The success of different approaches in the results obtained with different metrics shows how effective the selected metric is in measuring the segmented image quality. For this reason, the metric should be chosen according to which features are desired to be in the foreground in the segmented image. Table 5 shows a general review about results for three metrics. The average best number of 70 cases and the success rank of the methods are presented in Table 5.

Table 5. Average Best Number and Rank Values for Methods

	PSNR		SSIM		FSIM	
	#Best	Rank	#Best	Rank	#Best	Rank
Otsu	68	1	61	1	60	1
Kapur	0	3	0	4	7	4
Renyi	0	3	19	3	59	2
Tsallis	0	3	0	4	0	5
MCE	2	2	44	2	42	3
Shannon	0	3	0	4	0	5

DISCUSSION AND CONCLUSION

In this study, the MFO algorithm has been applied on 10 benchmark images which have different properties. The algorithm has been applied for seven different threshold levels. Six different threshold methods (Otsu, Kapur, Renyi, Tsallis, MCE and Shannon) have been used as the objective function. The performance of the thresholding methods have been compared with three different metrics (PSNR, SSIM and FSIM). According to the experimental results, it has been observed that the Otsu method is far more successful than other approaches. Especially in PSNR metric, Otsu method was quite successful than other approaches, while MCE approach increased its success in SSIM metric, Renyi approach came to the forefront together with Otsu in FSIM metric. Experimental results have shown that the selected thresholding method is directly effective in success. In addition, comparison metrics also reveal the measurement of success from different angles by handling segmented images with different features.

Considering the results, it is seen that the method used is quite effective in the segmentation process. In future studies, it can be investigated which thresholding approach is more suitable for which type of image by considering specific images. In addition, new approaches can be brought to the literature by being inspired by existing thresholding methods.

REFERENCES

- Abdel-Basset, M., Mohamed, R., AbdelAziz, N. M., & Abouhawwash, M. (2022). HWOA: A hybrid whale optimization algorithm with a novel local minima avoidance method for multi-level thresholding color image segmentation. *Expert Systems with Applications*, 190, 116145. <https://doi.org/10.1016/j.eswa.2021.116145>
- Bhandari, A. K., Kumar, A., & Singh, G. K. (2015a). Modified artificial bee colony based computationally efficient multilevel thresholding for satellite image segmentation using Kapur's, Otsu and Tsallis functions. *Expert Systems with Applications*, 42(3), 1573-1601. <https://doi.org/10.1016/j.eswa.2014.09.049>
- Bhandari, A. K., Kumar, A., & Singh, G. K. (2015b). Tsallis entropy based multilevel thresholding for colored satellite image segmentation using evolutionary algorithms. *Expert Systems with Applications*, 42(22), 8707-8730. <https://doi.org/10.1016/j.eswa.2015.07.025>
- Brooks, A. C., Zhao, X., & Pappas, T. N. (2008). Structural similarity quality metrics in a coding context: exploring the space of realistic distortions. *IEEE Transactions on image processing*, 17(8), 1261-1273. <https://doi.org/10.1109/TIP.2008.926161>
- Cai, Y., Mi, S., Yan, J., Peng, H., Luo, X., Yang, Q., & Wang, J. (2022). An unsupervised segmentation method based on dynamic threshold neural P systems for color images. *Information Sciences*, 587, 473-484. <https://doi.org/10.1016/j.ins.2021.12.058>
- Chen, Y., Wang, M., Heidari, A. A., Shi, B., Hu, Z., Zhang, Q., Chen, H., Mafarja, M., & Turabieh, H. (2022). Multi-threshold image segmentation using a multi-strategy shuffled frog leaping algorithm. *Expert Systems with Applications*, 194, 116511. <https://doi.org/10.1016/j.eswa.2022.116511> <https://doi.org/10.1016/j.eswa.2022.116511>
- De Albuquerque, M. P., Esquef, I. A., Mello, A. R. G., & De Albuquerque, M. P. (2004). Image thresholding using Tsallis entropy. *Pattern Recognition Letters*, 25(9), 1059-1065. <https://doi.org/10.1016/j.patrec.2004.03.003>
- Günay, M., & Taze, M. (2022). Mikroskopik Görüntülerde Multipl Miyelom Plazma Hücrelerinin Tespiti. *Kahramanmaraş Sütçü İmam Üniversitesi Mühendislik Bilimleri Dergisi*, 25(2), 145-154. <https://doi.org/10.17780/ksujes.1120829>

- Hore, A., & Ziou, D. (2010). Image quality metrics: PSNR vs. SSIM. Paper presented at the 2010 20th international conference on pattern recognition. <https://doi.org/10.1109/ICPR.2010.579>
- Houssein, E. H., Helmy, B. E., Oliva, D., Jangir, P., Premkumar, M., Elngar, A. A., & Shaban, H. (2022). An efficient multi-thresholding based COVID-19 CT images segmentation approach using an improved equilibrium optimizer. *Biomedical Signal Processing and Control*, 73, 103401. <https://doi.org/10.1016/j.bspc.2021.103401>
- Huang, C., Li, X., & Wen, Y. (2021). AN OTSU image segmentation based on fruitfly optimization algorithm. *Alexandria Engineering Journal*, 60(1), 183-188. <https://doi.org/10.1016/j.aej.2020.06.054>
- Ishak, A. B. (2017). A two-dimensional multilevel thresholding method for image segmentation. *Applied Soft Computing*, 52, 306-322. <https://doi.org/10.1016/j.asoc.2016.10.034>
- Kalyani, R., Sathya, P., & Sakthivel, V. (2020). Trading strategies for image segmentation using multilevel thresholding aided with minimum cross entropy. *Engineering Science and Technology, an International Journal*, 23(6), 1327-1341. <https://doi.org/10.1016/j.jestch.2020.07.007>
- Kapur, J. N., Sahoo, P. K., & Wong, A. K. (1985). A new method for gray-level picture thresholding using the entropy of the histogram. *Computer vision, graphics, and image processing*, 29(3), 273-285. [https://doi.org/10.1016/0734-189X\(85\)90125-2](https://doi.org/10.1016/0734-189X(85)90125-2)
- Karakoyun, M., Baykan, N. A., & Hacibeyoglu, M. (2017a). Multi-level thresholding for image segmentation with swarm optimization algorithms. *International Research Journal of Electronics & Computer Engineering*, 3(3), 1. <https://doi.org/10.24178/irjece.2017.3.3.01>
- Karakoyun, M., Gülcü, Ş., & Kodaz, H. (2021). D-MOSG: Discrete multi-objective shuffled gray wolf optimizer for multi-level image thresholding. *Engineering Science and Technology, an International Journal*, 24(6), 1455-1466. <https://doi.org/10.1016/j.jestch.2021.03.011>
- Karakoyun, M., & Özkiş, A. (2021). Transfer Fonksiyonları Kullanarak İkili Güve-Alev Optimizasyonu Algoritmalarının Geliştirilmesi ve Performanslarının Karşılaştırılması. *Necmettin Erbakan Üniversitesi Fen ve Mühendislik Bilimleri Dergisi*, 3(2), 1-10.
- Karakoyun, M., Sağlam, A., Baykan, N. A., & Altun, A. A. (2017b). Non-locally color image segmentation for remote sensing images in different color spaces by using data-clustering methods. *image*, 10, 11.
- Koc, I., Baykan, O. K., & Babaoglu, I. (2018). Multilevel image thresholding selection based on grey wolf optimizer. *JOURNAL OF POLYTECHNIC-POLITEKNIK DERGISI*, 21(4), 841-847. <https://doi.org/10.2339/politeknik.389613>
- Li, Y., Cao, G., Wang, T., Cui, Q., & Wang, B. (2020). A novel local region-based active contour model for image segmentation using Bayes theorem. *Information Sciences*, 506, 443-456. <https://doi.org/10.1016/j.ins.2019.08.021>
- Li, Y., Zhu, X., & Liu, J. (2020). An improved moth-flame optimization algorithm for engineering problems. *Symmetry*, 12(8), 1234. <https://doi.org/10.3390/sym12081234>
- Ma, G., & Yue, X. (2022). An improved whale optimization algorithm based on multilevel threshold image segmentation using the Otsu method. *Engineering Applications of Artificial Intelligence*, 113, 104960. <https://doi.org/10.1016/j.engappai.2022.104960>
- Mirjalili, S. (2015). Moth-flame optimization algorithm: A novel nature-inspired heuristic paradigm. *Knowledge-based systems*, 89, 228-249. <https://doi.org/10.1016/j.knsys.2015.07.006>
- Naidu, M., Kumar, P. R., & Chiranjeevi, K. (2018). Shannon and fuzzy entropy based evolutionary image thresholding for image segmentation. *Alexandria Engineering Journal*, 57(3), 1643-1655. <https://doi.org/10.1016/j.aej.2017.05.024>
- Otsu, N. (1979). A threshold selection method from gray-level histograms. *IEEE transactions on systems, man, and cybernetics*, 9(1), 62-66.
- Pal, N. R. (1996). On minimum cross-entropy thresholding. *Pattern recognition*, 29(4), 575-580. [https://doi.org/10.1016/0031-3203\(95\)00111-5](https://doi.org/10.1016/0031-3203(95)00111-5)
- Priyadharsini, R., & Sharmila, T. S. (2019). Object detection in underwater acoustic images using edge based segmentation method. *Procedia Computer Science*, 165, 759-765. <https://doi.org/10.1016/j.procs.2020.01.015>

- Raj, A., Gautam, G., Abdullah, S. N. H. S., Zaini, A. S., & Mukhopadhyay, S. (2019). Multi-level thresholding based on differential evolution and Tsallis Fuzzy entropy. *Image and Vision Computing*, 91, 103792. <https://doi.org/10.1016/j.imavis.2019.07.004>
- Ryalat, M. H., Dorgham, O., Tedmori, S., Al-Rahamneh, Z., Al-Najdawi, N., & Mirjalili, S. (2022). Harris hawks optimization for COVID-19 diagnosis based on multi-threshold image segmentation. *Neural Computing and Applications*, 1-19. <https://doi.org/10.1007/s00521-022-08078-4>
- Sahoo, P., Wilkins, C., & Yeager, J. (1997). Threshold selection using Renyi's entropy. *Pattern recognition*, 30(1), 71-84. [https://doi.org/10.1016/S0031-3203\(96\)00065-9](https://doi.org/10.1016/S0031-3203(96)00065-9)
- Sara, U., Akter, M., & Uddin, M. S. (2019). Image quality assessment through FSIM, SSIM, MSE and PSNR—a comparative study. *Journal of Computer and Communications*, 7(3), 8-18. <https://doi.org/10.4236/jcc.2019.73002>
- Satapathy, S. C., Sri Madhava Raja, N., Rajinikanth, V., Ashour, A. S., & Dey, N. (2018). Multi-level image thresholding using Otsu and chaotic bat algorithm. *Neural Computing and Applications*, 29(12), 1285-1307. <https://doi.org/10.1007/s00521-016-2645-5>
- Selçuk, T., Bilal, N., Sarıca, S., Akben, B., & Alkan, A. (2017). Ses Tellerinde Oluşan Nodüllere Ait Şekilsel Özelliklerin Görüntü İşleme Teknikleriyle Otomatik Olarak Belirlenmesi. *Kahramanmaraş Sütçü İmam Üniversitesi Mühendislik Bilimleri Dergisi*, 20(4), 54-59. <https://doi.org/10.17780/ksujes.349448>
- Shannon, C. E. (1948). A mathematical theory of communication. *The Bell system technical journal*, 27(3), 379-423. <https://doi.org/10.1002/j.1538-7305.1948.tb01338.x>
- Shehab, M., Abualigah, L., Al Hamad, H., Alabool, H., Alshinwan, M., & Khasawneh, A. M. (2020). Moth–flame optimization algorithm: variants and applications. *Neural Computing and Applications*, 32(14), 9859-9884. <https://doi.org/10.1007/s00521-019-04570-6>
- Tuba, E., Alihodzic, A., & Tuba, M. (2017). Multilevel image thresholding using elephant herding optimization algorithm. Paper presented at the 2017 14th international conference on engineering of modern electric systems (EMES). <https://doi.org/10.1109/EMES.2017.7980424>
- Wang, Z., Bovik, A. C., Sheikh, H. R., & Simoncelli, E. P. (2004). Image quality assessment: from error visibility to structural similarity. *IEEE Transactions on image processing*, 13(4), 600-612. <https://doi.org/10.1109/TIP.2003.819861>
- Xing, Z., & He, Y. (2021). Many-objective multilevel thresholding image segmentation for infrared images of power equipment with boost marine predators algorithm. *Applied Soft Computing*, 113, 107905. <https://doi.org/10.1016/j.asoc.2021.107905>
- Zhang, L., Zhang, L., Mou, X., & Zhang, D. (2011). FSIM: A feature similarity index for image quality assessment. *IEEE Transactions on image processing*, 20(8), 2378-2386. <https://doi.org/10.1109/TIP.2011.2109730>
- Zhao, S., Wang, P., Heidari, A. A., Chen, H., Turabieh, H., Mafarja, M., & Li, C. (2021). Multilevel threshold image segmentation with diffusion association slime mould algorithm and Renyi's entropy for chronic obstructive pulmonary disease. *Computers in Biology and Medicine*, 134, 104427. <https://doi.org/10.1016/j.compbiomed.2021.104427>